Available online at www.sciencedirect.com

SciVerse ScienceDirect

Ceramics International 39 (2013) 1901–1908

CERAMICS INTERNATIONAL

www.elsevier.com/locate/ceramint

Atmospheric pressure synthesis of Be- and Mg-doped $TlBa_2Ca_2Cu_3O_{10-\delta}$ superconductor

Nawazish A. Khan[a], M. Zubair[a], M. Mumtaz[a,b], A.A. Khurram[c,*]

[a]Materials Science Laboratory, Department of Physics, Quaid-i-Azam University, Islamabad 45320, Pakistan
[b]Materials Research Laboratory, Department of Physics, FBAS, International Islamic University Islamabad (IIUI), Islamabad 44000, Pakistan
[c]Experimental Physics Laboratories, National Centre for Physics, Islamabad, Pakistan

Received 5 August 2012; accepted 13 August 2012
Available online 18 August 2012

Abstract

We have doped Be and Mg at the Ca sites in $TlBa_2(Ca_{2-y}M_y)Cu_3O_{10-\delta}$ superconductors. The improvement of inter-plane coupling is most likely accomplished due to higher electro-negativity and smaller sizes of Be (1.5 Pauling, 1.12 Å) and Mg (1.2 Pauling, 1.6 Å) atoms in comparison with the Ca (1.0 Pauling, 1.97 Å) atom, whereas the suppression of anti-ferromagnetically aligned spins of copper atoms is achieved by making the distribution of carriers optimum and uniform in all CuO_2 planes. The influence of enhanced inter-plane coupling and reduced anti-ferromagnetism can be witnessed in the form of increased magnitude of diamagnetism in Be- and Mg-doped $TlBa_2(Ca_{2-y}M_y)Cu_3O_{10-\delta}$ samples as compared to un-doped $TlBa_2Ca_2Cu_3O_{10-\delta}$ samples. The increase in magnitude of the superconductivity with Be- and Mg-doping in $TlBa_2(Ca_{2-y}M_y)Cu_3O_{10-\delta}$ samples is less than that of previously studied Be- and Mg-doped $(Cu_{0.5}Tl_{0.5})Ba_2(Ca_{2-y}M_y)Cu_3O_{10-\delta}$ samples.

Keywords: Anti-ferromagnetism; Doping; Inter-plane coupling; $TlBa_2(Ca_{2-y}M_y)Cu_3O_{10-\delta}$ superconductor

1. Introduction

Cu-based superconductors like $CuBa_2Ca_2Cu_3O_{10-\delta}$ (Cu-1223) are the best choice in the cuprate family [1] because of their lower anisotropy ($\gamma=\rho_c/\rho_{ab}=H_{c\perp}/H_{c||}=\lambda_c/\lambda_{ab}=\xi_{ab}/\xi_c$), larger coherence length along the *c*-axis (ξ_c) and higher superconductivity parameters (such as T_c, J_c and H_c) [2]. In Cu-based compounds, the charge carriers have to tunnel the metallic Josephson barriers of $CuBa_2O_{4-\delta}$ charge reservoir layers during their transport along the *c*-axis. Therefore, lower resistivity is offered to the flow of carriers through $CuBa_2O_{4-\delta}$ charge reservoir layers of $CuBa_2Ca_2Cu_3O_{10-\delta}$ superconductor as compared to the flow of carriers through the insulating $TlBa_2O_{4-\delta}$ charge reservoir layer in $TlBa_2Ca_2Cu_3O_{10-\delta}$ (Tl-1223) superconductors [3]. However, the synthesis of Cu-based compounds at low pressure has not yet become possible; the Cu-1223 superconductor can be synthesized under a 4.2 GPa high pressure [4,5]. The intermediate CuTl-based superconductors like $(Cu_{0.5}Tl_{0.5})Ba_2Ca_2Cu_3O_{10-\delta}$ (CuTl-1223) have partially conducting and partially insulating $(Cu_{0.5}Tl_{0.5})Ba_2O_{4-\delta}$ charge reservoir layers and their superconducting properties are as good as in the Cu-based superconductors [6]. In a previous study, we have doped smaller sized Be and Mg atoms at Ca sites in the CuTl-1223 superconductor to enhance the inter-plane coupling and to reduce the anisotropy along the *c*-axis to improve the superconductivity [7,8]. In the present study, we have doped Be and Mg atoms at the Ca sites in the Tl-1223 superconductor. The main motivation behind this study was to improve the superconductivity in Tl-1223 samples and to compare the role of insulating the $TlBa_2O_{4-\delta}$ charge reservoir layer of the Tl-1223 superconductor with the partially insulating $(Cu_{0.5}Tl_{0.5})Ba_2O_{4-\delta}$ charge reservoir layer of the CuTl-1223 superconductor in the charge transport processes. The superconductivity mechanism in Tl-1223 is identical to that in Cu-1223 and in CuTl-1223 superconductors i.e. they have charge reservoir layers and conducting CuO_2 planes [9]. The doping

*Corresponding author. Tel.: +92 51 2896086; fax: +92 51 2896084.
E-mail address: khuram_qau@yahoo.com (A.A. Khurram).

0272-8842/$ - see front matter © 2012 Elsevier Ltd and Techna Group S.r.l. All rights reserved.
http://dx.doi.org/10.1016/j.ceramint.2012.08.039

efficiency of the $TlBa_2O_{4-\delta}$ charge reservoir layer in the Tl-1223 superconductor can be estimated by carrying out post-annealing experiments on these samples in oxygen flow [10]. The intercalation of oxygen (O_δ) in the charge reservoir layer controls the flow of carriers towards the conducting CuO_2 planes i.e. an optimum amount of O_δ would help the electrons to flow towards the conducting CuO_2 planes [11]. Intercalation of O_δ in the Tl-1223 superconductor after oxygen post annealing can be estimated from FTIR absorption measurements through the relative comparison of intensity of O_δ modes around 690 cm^{-1} in the as-prepared samples and in post-annealed samples [12].

Moreover, in Tl-1223 superconductors, there are three inequivalent CuO_2 planes as far as the charge carrier concentration is concerned [5]. The outer CuO_2 planes (OP), which are directly connected to the charge reservoir layer, are over-doped with carriers, whereas the inner CuO_2 planes (IP) have an under-doped carrier concentration [5]. It has been well established by many experiments that Tl-based compounds with more than two CuO_2 planes have lower density of mobile carriers, which promotes anti-ferromagnetic alignment of small spins of Cu atoms. The existence of such anti-ferromagnetically aligned spins of the copper atoms in CuO_2 planes suppresses the over-all superconducting properties of these compounds.

The smaller magnetic moments of Cu atoms get anti-ferromagnetic aligned spin arrangement due to the smaller density of the carriers in IP to minimize their energy [13]. The existence of anti-ferromagnetism in the IP suppresses the over-all superconducting properties of materials [14,15]. The substitution of Be and Mg at Ca sites improves the inter-plane coupling and promotes the uniform distribution of carriers in the OP and IP and in turn suppresses anti-ferromagnetism, which would help in enhancing the superconducting properties of materials [7–8].

2. Experimental

Superconducting $TlBa_2(Ca_{2-y}M_y)Cu_3O_{10-\delta}$ (M = Mg, and Be; $y = 0$, 0.25, 0.5, 0.75, and 1.0) samples were prepared by the solid state reaction method accomplished in two stages. At the first stage $Ba_2(Ca_{2-y}M_y)Cu_3O_{10-\delta}$ precursor material was prepared by thoroughly mixing $Ba(NO_3)_2$, $Ca(NO_3)_2$, MgO/BeO and Cu(CN) compounds in a quartz mortar and pestle in appropriate ratios. The mixed material loaded in a quartz boat was fired twice at 860 °C for 24 h in a preheated furnace. After the 24 h heat treatment, the furnace was switched off and the precursor material was cooled down to room temperature. At the second stage, thallium oxide (Tl_2O_3) was mixed with precursor material and was ground for about 1 h. The Tl_2O_3 mixed material was palletized under 3.8 t/cm^2 pressure and the pellets were enclosed in gold capsules. The pellets enclosed in gold capsules were sintered at 860 °C for about 10 min and then quenched to room temperature. The samples were characterized by dc-resistivity and ac-susceptibility measurements. The structure of the material was determined by X-ray diffraction (XRD) scan from Brouker X-ray diffractometer using a CuKα source of wavelength 1.54056 Å and the cell parameters were calculated using the cell refinement computer program. The oxygen phonon modes in the $TlBa_2(Ca_{2-y}M_y)Cu_3O_{10-\delta}$ unit cell were observed by a Nicolet 5700 Fourier Transform Infrared Spectrometer (FTIR) in a 400–700 cm^{-1} wavenumber range. The post-annealing experiments on these samples were carried out in flowing oxygen in a tubular furnace at 500 °C for 6 h.

3. Results and discussion

3.1. As-prepared Mg-doped $TlBa_2(Ca_{2-y}Mg_y)Cu_3O_{10-\delta}$ samples

The resistivity vs temperature measurements of Mg-doped $TlBa_2(Ca_{2-y}Mg_y)Cu_3O_{10-\delta}$ ($y = 0$, 0.25, 0.5, 0.75, and 1.0) samples are shown in Fig. 1. The variation of resistivity remains metallic from room temperature down to the onset of superconductivity for all samples. The room temperature resistivity in these samples varies from 0.022 to 0.040 Ω cm. These samples showed onset of superconductivity (T_c^{onset}) at around 113, 122, 121, 120, and 119 K and zero resistivity critical temperatures $\{T_c(R=0)\}$ of around 102, 105, 114, 103, and 101 K for $y = 0$, 0.25, 0.5, 0.75, and 1.0 respectively. Initially $T_c(R=0)$ increases with Mg-doping up to $y = 0.5$ and then starts to decrease beyond $y > 0.5$.

The ac-susceptibility vs temperature measurements of $TlBa_2(Ca_{2-y}Mg_y)Cu_3O_{10-\delta}$ ($y = 0$, 0.25, 0.5, 0.75, and 1.0) samples are shown in Fig. 2. The magnitude of diamagnetism increases with Mg-doping, which is possibly due to improved inter-plane coupling and optimization of carrier concentration in the CuO_2 planes. The smaller sized Mg as compared to Ca improves the inter-plane coupling and decreases the volume of the unit cell due to which the

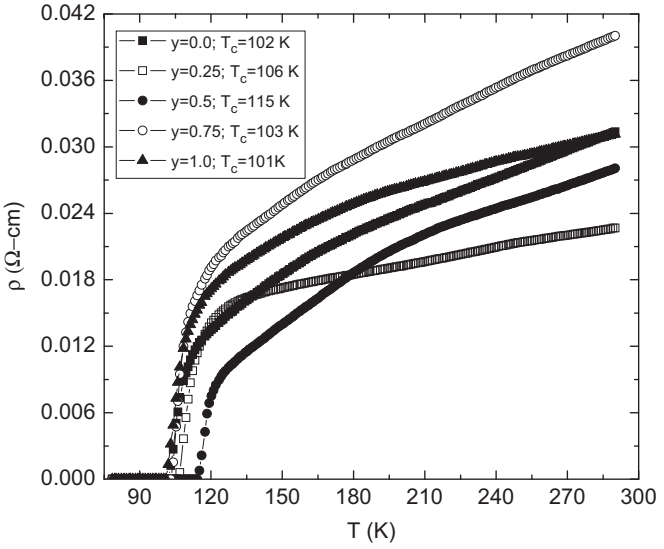

Fig. 1. Resistivity vs temperature curves of the as-prepared $TlBa_2(Ca_{2-y}Mg_y)Cu_3O_{10-\delta}$ ($y = 0$, 0.25, 0.5, 0.75, and 1.0) superconductors.

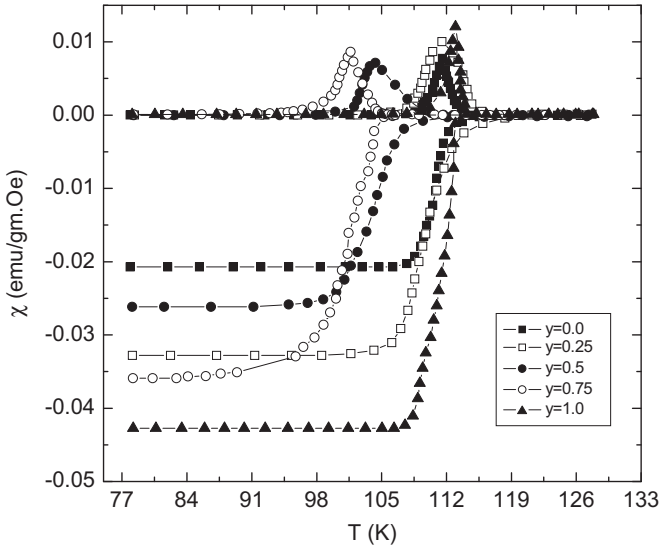

Fig. 2. Ac-susceptibility vs temperature measurements of the as-prepared $TlBa_2(Ca_{2-y}Mg_y)Cu_3O_{10-\delta}$ ($y=0$, 0.25, 0.5, 0.75, and 1.0) superconductors.

carrier density becomes optimum in CuO_2 planes. The magnitude of anti-ferromagnetically aligned moments of small spins of Cu atoms in IP is also suppressed due to increased density of carriers resulting in an increase in superconductivity of the material.

The FTIR absorption measurements of $TlBa_2(Ca_{2-y}Mg_y)Cu_3O_{10-\delta}$ ($y=0$, 0.25, 0.5, 0.75, and 1.0) samples are shown in Fig. 3. In CuTl-1223 samples, the modes of vibration related to the apical oxygen atoms are observed at around 400–540 cm^{-1}, CuO_2 planar oxygen atoms at around 540–600 cm^{-1} and O_δ atoms in the $Cu_{0.5}Tl_{0.5}Ba_2O_{4-\delta}$ charge reservoir layer at around 660–700 cm^{-1} [10,16]. In Mg free Tl-1223 samples, only the single apical oxygen mode of type Tl-O_A-Cu(2) was expected to be observed and this mode is observed at 547 cm^{-1}. The CuO_2 planar oxygen mode is observed at around 607 cm^{-1} and the O_δ mode of oxygen atoms in $TlBa_2O_{4-\delta}$ charge reservoir layer is peaked at around 694 cm^{-1}. The intensity of this apical oxygen mode and O_δ mode of oxygen atoms decreases, whereas the intensity of the CuO_2 planar oxygen mode observed at around 594–607 cm^{-1} increases with increase of Mg-doping in $TlBa_2(Ca_{2-y}Mg_y)Cu_3O_{10-\delta}$ samples. The decrease in the intensity of the O_δ mode indicates that the oxygen content has been decreased with increase of Mg-doping in $TlBa_2(Ca_{2-y}Mg_y)Cu_3O_{10-\delta}$ samples. The CuO_2 planar oxygen mode is systematically softened with the increase of Mg-doping and is observed at around 607, 604, 594, 596 and 594 cm^{-1} for $y=0$, 0.25, 0.5, 0.75, and 1.0, respectively.

The X-ray diffraction (XRD) scans of $TlBa_2(Ca_{2-y}Mg_y)Cu_3O_{10-\delta}$ ($y=0$, 0.75, and 1.5) samples are shown in Fig. 4. Most of the diffraction lines are indexed according to the tetragonal structure by following the P4/mmm space group. The cell parameters calculated using these planar reflections have shown a decreasing trend i.e. both *a*- and *c*-axes lengths have been decreased with Mg-doping at the Ca sites.

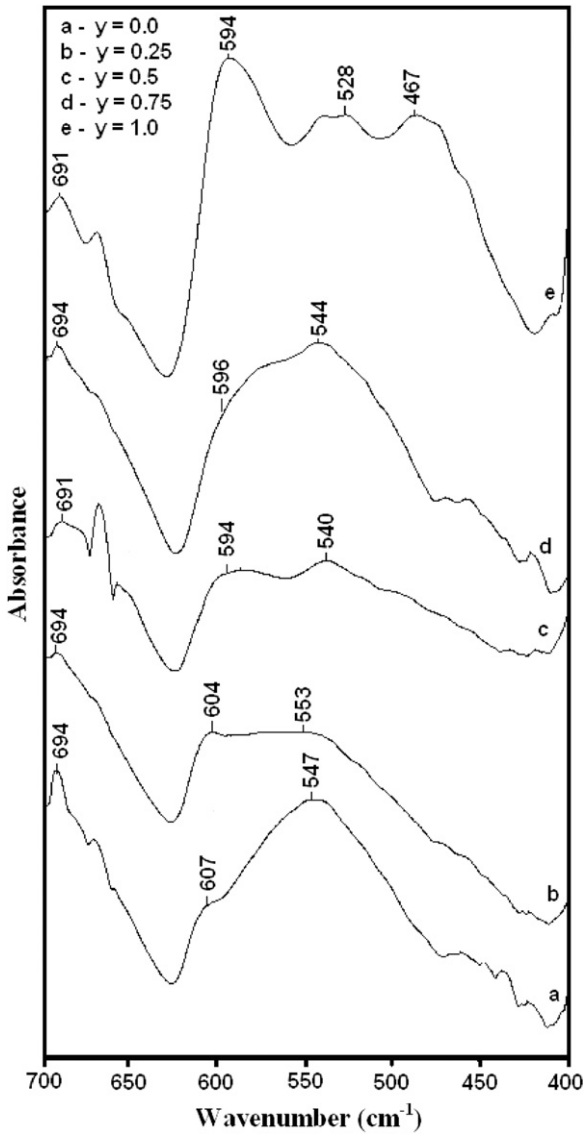

Fig. 3. FTIR absorption spectra of the as-prepared $TlBa_2(Ca_{2-y}Mg_y)Cu_3O_{10-\delta}$ ($y=0$, 0.25, 0.5, 0.75, and 1.0) superconductors.

3.2. *Oxygen post-annealed Mg-doped $TlBa_2(Ca_{2-y}Mg_y)Cu_3O_{10-\delta}$ samples*

The resistivity verses temperature measurements of oxygen annealed $TlBa_2(Ca_{2-y}Mg_y)Cu_3O_{10-\delta}$ ($y=0$, 0.25, 0.5, 0.75, and 1.0) samples are shown in Fig. 5. The annealed samples have also shown metallic variation of resistivity from room temperature down to onset of superconductivity. The room temperature resistivity in oxygen post-annealed samples is found to vary from 0.016 to 0.072 Ω cm. A significant increase in T_c^{onset} has been observed in Mg free samples, whereas it has been marginally improved with Mg-doping (i.e. $y=0.25$, 0.5, and 1.0). The $T_c(R=0)$ has also been marginally improved in these samples.

The ac-susceptibility measurements of oxygen post-annealed $TlBa_2(Ca_{2-y}Mg_y)Cu_3O_{10-\delta}$ samples are shown in Fig. 6. In comparison with the as-prepared samples, an improvement in the magnitude of diamagnetism could be witnessed in all

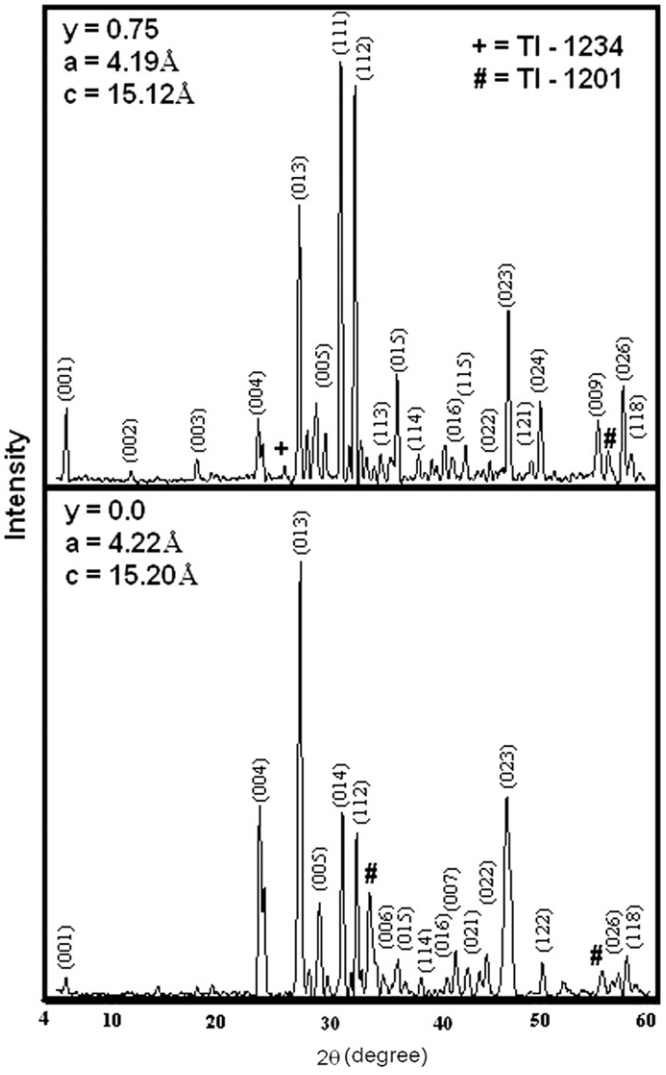

Fig. 4. XRD patterns of $TlBa_2(Ca_{2-y}Mg_y)Cu_3O_{10-\delta}$ ($y=0$ and 0.75) superconductors.

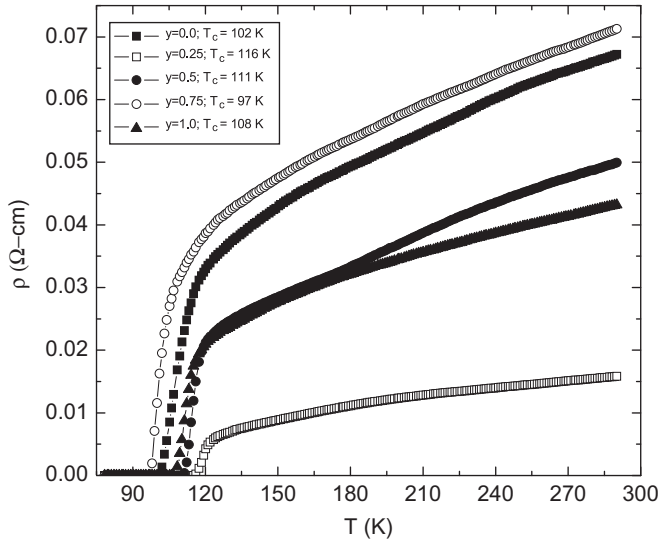

Fig. 5. Resistivity vs temperature curves of O_2 post-annealed $TlBa_2(Ca_{2-y}Mg_y)Cu_3O_{10-\delta}$ ($y=0$, 0.25, 0.5, 0.75, and 1.0) superconductors.

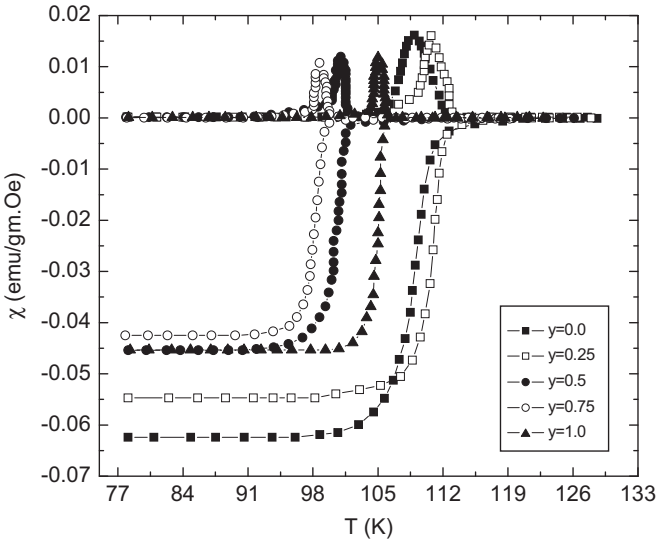

Fig. 6. Ac-susceptibility vs temperature measurements of O_2 post-annealed $TlBa_2(Ca_{2-y}Mg_y)Cu_3O_{10-\delta}$ ($y=0$, 0.25, 0.5, 0.75, and 1.0) superconductors.

oxygen post-annealed samples. It is most likely that oxygen optimization in the unit cell promotes the improvement of superconducting properties of $TlBa_2(Ca_{2-y}Mg_y)Cu_3O_{10-\delta}$ samples in terms of increased magnitude of diamagnetism.

The FTIR absorption measurements of oxygen post-annealed $TlBa_2(Ca_{2-y}Mg_y)Cu_3O_{10-\delta}$ samples are shown in Fig. 7. In Mg free Tl-1223 samples, the apical oxygen mode of the type Tl-O_A-Cu(2) is observed at around 546 cm^{-1}. The CuO_2 planar oxygen mode is observed at around 596 cm^{-1} and the O_δ mode of oxygen in the $TlBa_2O_{4-\delta}$ charge reservoir layer is peaked at around 692 cm^{-1}. The intensity of the O_δ mode of the charge reservoir layer is increased after post-annealing in oxygen. The increased intensity of the O_δ mode in the $TlBa_2O_{4-\delta}$ charge reservoir layer at around 692 cm^{-1} shows the increased oxygen diffusion in the unit cell after oxygen post-annealing. The diffusion of oxygen takes place not only at inter-granular sites but also on intra-granular sites, which increases the grain size, inter-grain connectivity and carrier density in CuO_2 planes. The CuO_2 planar oxygen modes are observed at around 596, 591, 577, 570, and 572 cm^{-1} for $y=0$, 0.25, 0.5, 0.75, and 1.0, respectively. The apical oxygen mode of the type Tl-O_A-Cu(2) for $y=0$, 0.25, 0.5, 0.75, and 1.0 have been observed at around 546,549, 534, 545, and 536 cm^{-1}, respectively. The softening of apical oxygen mode of type Tl-O_A-Cu(2) showed the enhanced inter-plane coupling.

3.3. *As-prepared Be-doped $TlBa_2(Ca_{2-y}Be_y)Cu_3O_{10-\delta}$ samples*

The resistivity vs temperature measurements of the as-prepared Be-doped $TlBa_2(Ca_{2-y}Be_y)Cu_3O_{10-\delta}$ ($y=0$, 0.25, 0.5, 0.75, and 1.0) samples are shown in Fig. 8. The resistivity variation as a function of temperature from

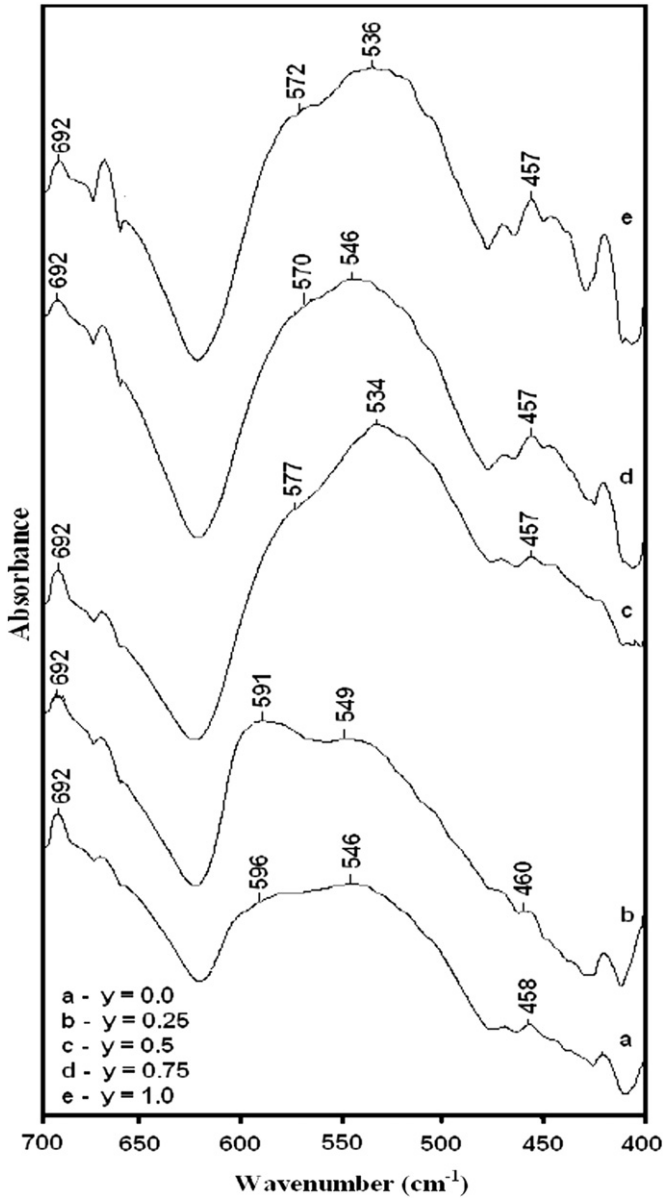

Fig. 7. FTIR absorption spectra of O_2 post-annealed $TlBa_2(Ca_{2-y}Mg_y)Cu_3O_{10-\delta}$ ($y=0$, 0.25, 0.5, 0.75, and 1.0) superconductors.

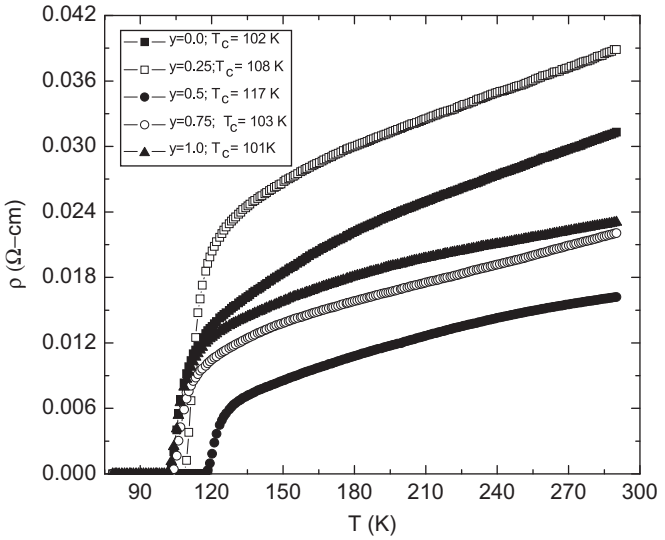

Fig. 8. Resistivity vs temperature curves of the as-prepared $TlBa_2(Ca_{2-y}Be_y)Cu_3O_{10-\delta}$ ($y=0$, 0.25, 0.5, 0.75, and 1.0) superconductors.

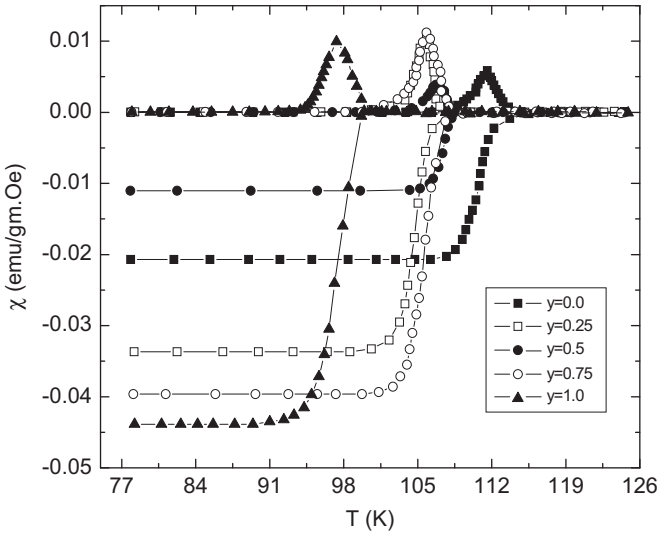

Fig. 9. Ac-susceptibility vs temperature measurements of the as-prepared $TlBa_2(Ca_{2-y}Be_y)Cu_3O_{10-\delta}$ ($y=0$, 0.25, 0.5, 0.75, and 1.0) superconductors.

room temperature down to the onset of superconductivity is metallic for all un-doped and Be-doped the samples. The variation of room temperature resistivity in these samples is observed between 0.016 and 0.0.39 Ω cm. The T_c^{onset} has been observed around 117, 124, 125, 113, 117 K and $T_c(R=0)$ around 102, 108, 117, 103, 102 K in $TlBa_2(Ca_{2-y}Be_y)Cu_3O_{10-\delta}$ samples for $y=0$, 0.25, 0.5, 0.75, and 1.0 respectively. A maximum enhancement in T_c^{onset} and $T_c(R=0)$ has been observed in the samples with $y=0.5$.

The ac-susceptibility measurements of $TlBa_2(Ca_{2-y}Be_y)Cu_3O_{10-\delta}$ samples are shown in Fig. 9. The magnitude of superconductivity increases with Be-doping in $TlBa_2(Ca_{2-y}Be_y)Cu_3O_{10-\delta}$ samples. The possible source of increasing diamagnetism is optimization of carriers in CuO_2 planes and inter-plane coupling due to the smaller size of Be as compared to that of the Ca atom. The Be substitution leads to suppression of volume of the unit cell resulting in an increase in the Fermi vector and coherence length along the anisotropic *c*-axis.

The FTIR absorption measurements of $TlBa_2(Ca_{2-y}Be_y)Cu_3O_{10-\delta}$ samples are shown in Fig. 10. In Be free Tl-1223 samples, the apical oxygen mode of the type Tl-O_A-Cu(2) has been observed at around 547 cm^{-1}. The CuO_2 planar oxygen mode is observed at around 607 cm^{-1} and the O_δ oxygen mode in the $TlBa_2O_{4-\delta}$ charge reservoir layer is peaked at around 694 cm^{-1}. Apical oxygen modes are observed at around 547, 546, 546, 545, and 549 cm^{-1} in the samples with $y=0$, 0.25, 0.5, 0.75, and 1.0, respectively. CuO_2 planar oxygen modes are observed at around 607, 590, 603, 589, and 593 cm^{-1} for $y=0$, 0.25, 0.5, 0.75, and 1.0, respectively. The apical oxygen mode of the type Tl-O_A-Cu(2)

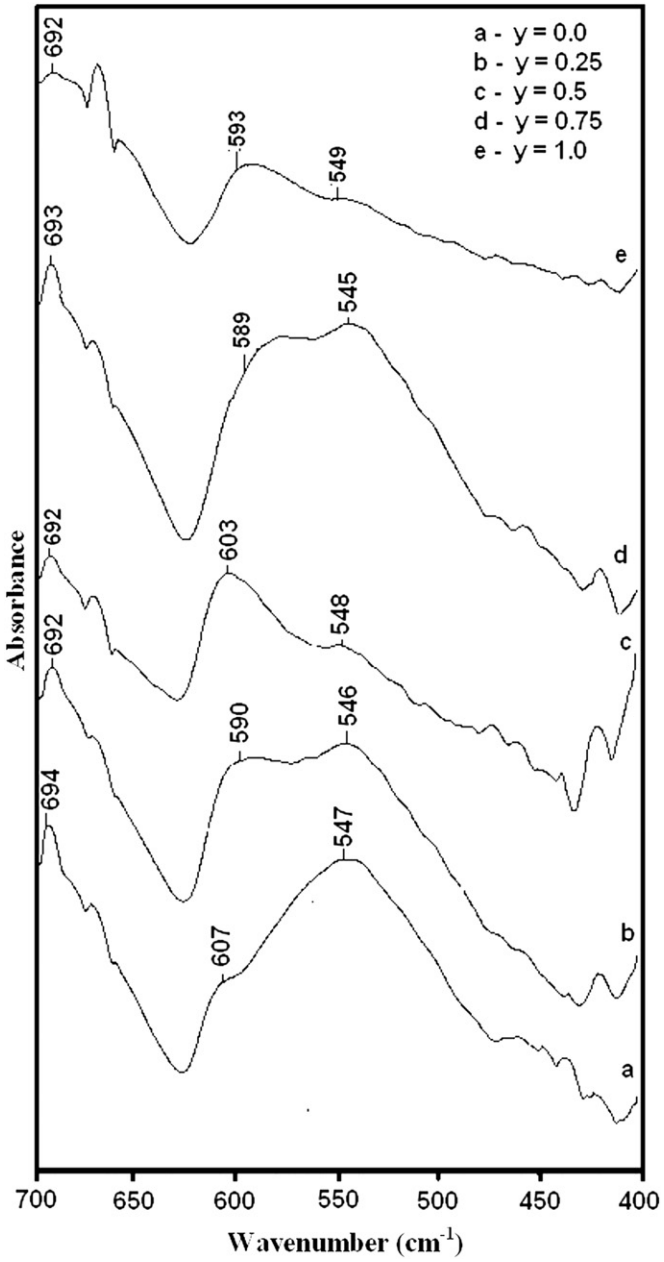

Fig. 10. FTIR absorption spectra of the as-prepared $TlBa_2(Ca_{2-y}Be_y)Cu_3O_{10-\delta}$ (y=0, 0.25, 0.5, 0.75, and 1.0) superconductors.

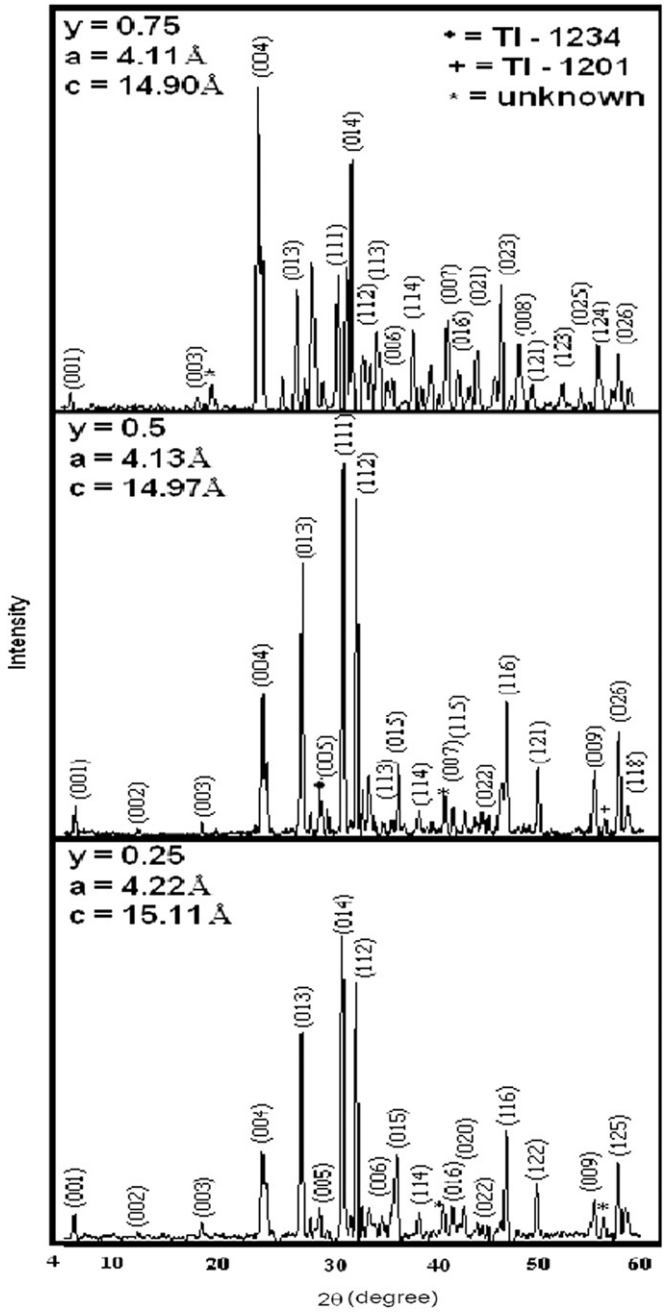

Fig. 11. XRD patterns of $TlBa_2(Ca_{2-y}Be_y)Cu_3O_{9-\delta}$ (y=0.25, 0.5, and 0.75) superconductors.

is also softened with the increased Be-doping in $TlBa_2(Ca_{2-y}Be_y)Cu_3O_{10-\delta}$ samples.

The X-ray diffraction scans (XRD) of $TlBa_2(Ca_{2-y}Be_y)Cu_3O_{10-\delta}$ (y=0.25, 0.5, and 0.75) samples are shown in Fig. 11. The planar reflections are indexed according to the tetragonal structure following the P4/mmm space group. The *a*- and *c*-axes lengths of the unit cell are calculated by using the planar reflections and it has been observed that *a*- and *c*-axes lengths both decrease with increase of Be-doping at the Ca sites in $TlBa_2(Ca_{2-y}Be_y)Cu_3O_{10-\delta}$ samples. Like Mg-doped $TlBa_2(Ca_{2-y}Mg_y)Cu_3O_{10-\delta}$ samples, these Be-doped $TlBa_2(Ca_{2-y}Be_y)Cu_3O_{10-\delta}$ samples have also shown an enhancement in the inter-plane coupling due to which the coherence length increases, anisotropy decreases, Fermi-vector increases and carrier density becomes optimum.

3.4. Oxygen post-annealed Be-doped $TlBa_2(Ca_{2-y}Be_y)Cu_3O_{10-\delta}$ samples

The resistivity vs temperature measurements of oxygen post-annealed Be-doped $TlBa_2(Ca_{2-y}Be_y)Cu_3O_{10-\delta}$ samples are shown in Fig. 12. These samples have also shown metallic behavior of resistivity variation from room temperature down to the onset of superconductivity. The

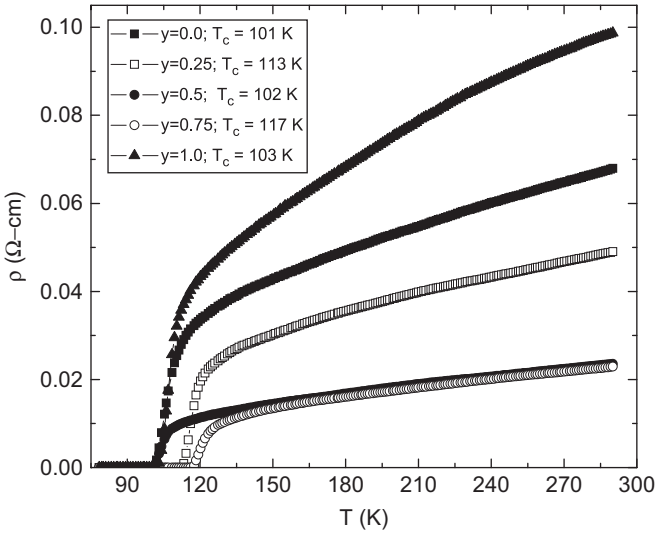

Fig. 12. Resistivity vs temperature curves of O_2 post-annealed $TlBa_2(Ca_{2-y}Be_y)Cu_3O_{10-\delta}$ (y=0, 0.25, 0.5, 0.75, and 1.0) superconductors.

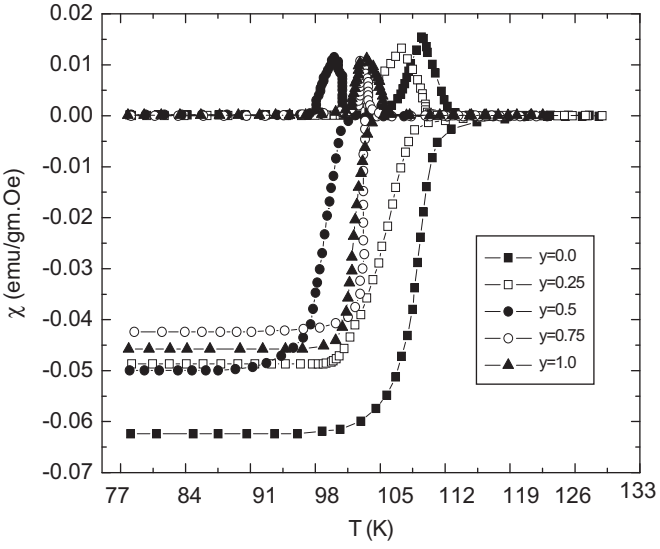

Fig. 13. Ac-susceptibility vs temperature measurements of O_2 post-annealed $TlBa_2(Ca_{2-y}Be_y)Cu_3O_{10-\delta}$ (y=0, 0.25, 0.5, 0.75, and 1.0) superconductors.

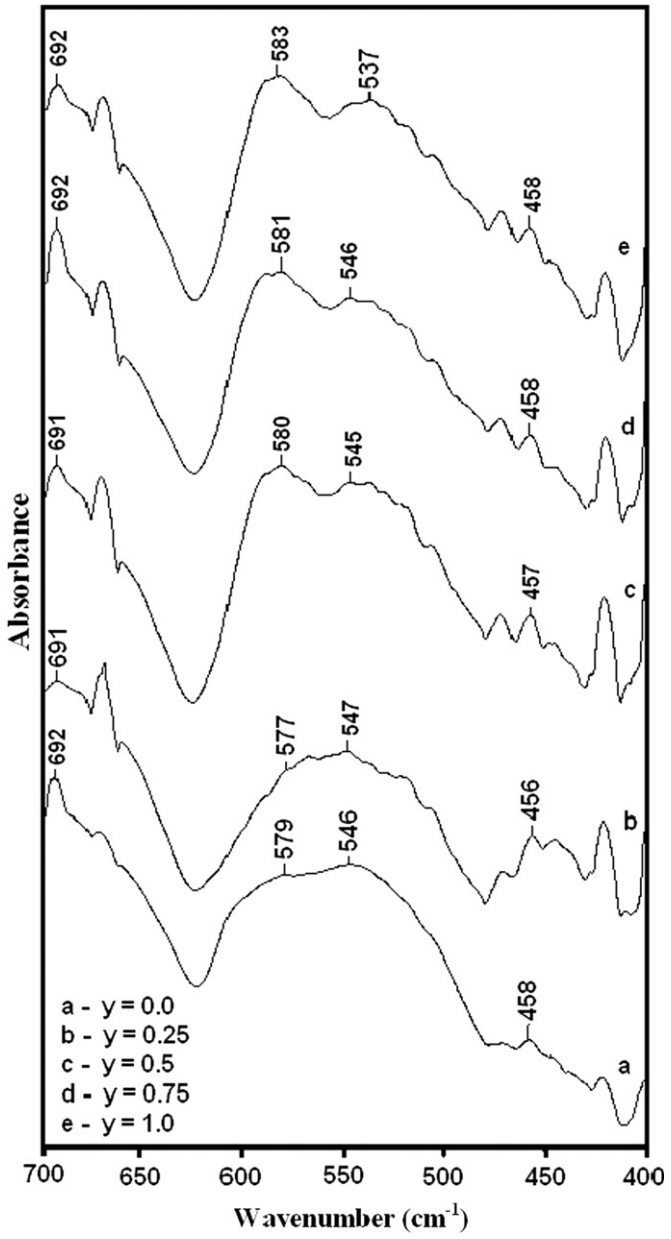

Fig. 14. FTIR absorption spectra of O_2 post-annealed $TlBa_2(Ca_{2-y}Be_y)Cu_3O_{10-\delta}$ (y=0, 0.25, 0.5, 0.75, and 1.0) superconductors.

room temperature resistivity in these samples varies in the range from 0.023 to 0.098 Ω cm.

The ac-susceptibility measurements of oxygen post-annealed $TlBa_2(Ca_{2-y}Be_y)Cu_3O_{10-\delta}$ samples are shown in Fig. 13. The magnitude of diamagnetism has been significantly suppressed in comparison with Be free Tl-1223 samples. It is most likely that oxygen post-annealing may push the material towards the over-doped regime, due to which superconductivity has been suppressed.

The FTIR absorption measurements of oxygen post-annealed $TlBa_2(Ca_{2-y}Be_y)Cu_3O_{10-\delta}$ samples are shown in Fig. 14. In Be free Tl-1223 samples, the apical oxygen mode of type Tl-O_A-Cu(2) has been observed at around 546 cm^{-1}, the CuO_2 planar oxygen mode at around 578 cm^{-1} and the O_δ oxygen mode in the $TlBa_2O_{4-\delta}$ charge reservoir layer at around 692 cm^{-1}. The intensity of the O_δ oxygen mode stays un-changed, which shows small intercalation of oxygen after oxygen post-annealing. The apical oxygen mode of type Tl-O_A-Cu(2) has been observed at around 547,545, 546, and 537 cm^{-1} for y=0.25, 0.5, 0.75, and 1.0, respectively. The CuO_2 planar oxygen modes are observed at around 577, 580, 581, and 583 cm^{-1} for y=0.25, 0.5, 0.75, and 1.0, respectively. The softening of apical oxygen mode and hardening of the CuO_2 planar oxygen mode is the manifestation of enhanced inter-plane coupling with Be-doping at Ca sites in the Tl-1223 superconductor.

4. Conclusions

We have synthesized Be- and Mg-doped $TlBa_2(Ca_{2-y}M_y)Cu_3O_{10-\delta}$ (M = Mg, and Be; y = 0, 0.25, 0.5, 0.75, 1.0, and 1.5) samples at ambient pressure for the first time and studied their superconducting properties. The X-ray diffraction (XRD) analysis has shown that the c-axis length has decreased with Be- and Mg-doping in the $TlBa_2(Ca_{2-y}M_y)Cu_3O_{10-\delta}$ superconductor (i.e. carrier's density has been enhanced $n \sim N/V$). The oxygen phonon modes observed by FTIR absorption spectroscopy have shown that distance among the CuO_2 planes has decreased with increased concentration of Be- and Mg-doping. These observations have shown the improvement in coupling strength of the CuO_2 plane with Be- and Mg-doping, which can be witnessed in the form of increased magnitude of diamagnetism in Be- and Mg-doped $TlBa_2(Ca_{2-y}M_y)Cu_3O_{10-\delta}$ samples. The marginal improvement in the superconducting properties of $TlBa_2(Ca_{2-y}M_y)Cu_3O_{10-\delta}$ samples with Be- and Mg-doping have unequivocally confirmed the better doping efficiency of the $(Cu_{0.5}Tl_{0.5})Ba_2O_{4-\delta}$ charge reservoir layer of $(Cu_{0.5}Tl_{0.5})Ba_2(Ca_{2-y}M_y)Cu_3O_{10-\delta}$ superconductors compared to the totally insulating $TlB_2O_{4-\delta}$ charge reservoir layer of $TlBa_2(Ca_{2-y}M_y)Cu_3O_{10-\delta}$ superconductors.

References

[1] Y. Kodama, A. Iyo, M. Hirai, H. Kito, Y. Tanaka, Annealing study of superconducting properties in a Cu-1223 superconductor using O_2-HIP apparatus, Physica C 392 (2003) 77.

[2] H. Ihara, A. Iyo, K. Tanaka, K. Tokiwa, K. Ishida, N. Terada, M. Tokumoto, Y. Sekita, T. Tsukamoto, T. Watanabe, M. Umeda, How to make superconducting-anisotropy least in high-T_c cuprate superconductors, Physica C 282 (1997) 1973.

[3] H. Kotegawa, Y. Tokunaga, K. Ishida, G.-q. Zheng, Y. Kitaoka, K. Asayama, H. Kito, A. Iyo, H. Ihara, K. Tanaka, K. Tokiwa, T. Watanabe, NMR study of carrier distribution and superconductivity in multilayered high-T_c cuprates, Journal of Physics and Chemistry of Solids 62 (2001) 171.

[4] K. Tokiwa, H. Aota, C. Kunugi, K. Tanaka, Y. Tanaka, A. Iyo, H. Ihara, T. Watanabe, Pressure effect on T_c in $(Cu,Tl)Ba_2Ca_2Cu_3O_y$ superconductor, Physica B 284 (2000) 1077.

[5] T. Watanabe, S. Miyashita, N. Ichioka, K. Tokiwa, K. Tanaka, A. Iyo, Y. Tanaka, H. Ihara, Carrier doping and superconducting properties in Cu-1234 and CuTl-1223 superconductors, Physica B 284 (2000) 1075.

[6] Nawazish A. Khan, Faish-ud-din, A.A. Khurram, Normal pressure synthesis of $Cu_{1-x}Tl_xBa_2Ca_2Cu_3O_{10-\delta}$ superconductor, Physica C 417 (2005) 119.

[7] Nawazish A. Khan, A.A. Khurrum, Enhanced superconducting properties of $Cu_{1-x}Tl_xBa_2Ca_{2-y}Mg_yCu_3O_{10-d}$.$y$=0, 0.5, 1.0, and 1.5, Applied Physics Letters 86 (2005) 152502.

[8] Nawazish A. Khan, G. Husnain, Superconductivity in Be substituted by Ca in $Cu_{0.5}Tl_{0.5}Ba_2Ca_{n-1-y}Be_yCu_nO_{2n+4-\delta}$ (n=3, 4 and y=0.7, 1.5, 1.7, 2.0), Physica C 436 (2006) 51.

[9] H. Ihara, K. Tanaka, Y. Tanaka, A. Iyo, N. Terada, M. Tokumoto, M. Ariyama, I. Hase, A. Sundaresan, N. Hamada, S. Miyashita, K. Tokiwa, T. Watanabe, Mechanism of T_c enhancement in $Cu_{1-x}Tl_x$-1234 and -1223 systems with $T_c > 130$ K, Physica C 341 (2000) 487.

[10] Nawazish A. Khan, A.A. Khurram, M. Mazhar, Effects of post-annealing on the infrared active phonon modes of low anisotropy (γ=5–11) $Cu_{1-x}Tl_xBa_2Ca_2Cu_3O_{10-\delta}$ superconductor thin films, Physica C 407 (2004) 23.

[11] Nawazish A. Khan, A.A. Khurram, A. Maqsood, Doping of the CuO_2 planes of $Cu_{1-x}Tl_xBa_2Ca_2Cu_3O_{10-y}$ superconductor via light and heavier ions, Physica C 398 (2003) 114.

[12] Nawazish A. Khan, M. Mumtaz, K. Sabeeh, M.I.A. Khan, Mushtaq Ahmed, The study of phonon modes of $Cu_{1-x}Tl_xBa_2Ca_3Cu_4O_{12-y}$ superconductor thin films by FTIR absorption spectroscopy, Physica C 407 (2004) 103.

[13] H. Kotegawa, Y. Tokunaga, K. Ishida, G.-q. Zheng, Y. Kitaoka, H. Kito, A. Iyo, K. Tokiwa, T. Watanabe, H. Ihara, Unusual magnetic and superconducting characteristics in multilayered high-T_c cuprates: ^{63}Cu NMR study, Physical Review B 64 (2001) 064515.

[14] Nawazish A Khan, M. Mumtaz, Homogeneous distribution of carriers in the conducting planes by Zn substitution at Cu sites in $Cu_{0.5}Tl_{0.5}Ba_2Ca_3Cu_4O_{12-d}$ superconductors, low temperature, Physica 36 (2010) 196.

[15] M. Mumtaz, Nawazish A. Khan, Reduced anti-ferromagnetism promoted by Zn $3d^{10}$ substitution at CuO_2 planar sites of $Cu_{0.5}Tl_{0.5}Ba_2Ca_3Cu_4O_{12-\delta}$ superconductors, Physica B 404 (2009) 3973.

[16] M. Irfan, Nawazish A. Khan, Study of phonon modes and superconducting properties of the oxygen post-annealed $(Cu_{0.5}Tl_{0.5})Ba_2Ca_{n-1}(Cu_{n-y}Ge_y)O_{2n+4-\delta}$ (n=3, 4 and y=0, 0.5, 0.75, 1.0) superconductors, Cyrogenics 50 (2010) 61.